Available online at www.sciencedirect.com
SCIENCE DIRECT
Journal of Sound and Vibration 293 (2006) 995–1006
JOURNAL OF SOUND AND VIBRATION
www.elsevier.com/locate/jsvi

Directivity of railway noise sources

Xuetao Zhang*, Hans G. Jonasson

SP Swedish National Testing and Research Institute, P.O. Box 857, SE-501 15 Borås, Sweden

Accepted 26 August 2005
Available online 8 February 2006

Abstract

In the Harmonoise project the description of vertical and horizontal directivities of railway noise sources has been required. Other features of the source description are sound power level spectra in one-third octave bands as a function of speed and the physical location of the different sound sources.

Based on systematic investigations methods to measure and to determine the directivities of railway noise sources are presented in this paper. The determination of the directivity of rolling noise is discussed in detail. For the directivities of traction noise and aerodynamic noise the discussion is more analytical because of limited access to relevant data.

For each type of main railway noise source, i.e. rolling noise, traction noise and aerodynamic noise, default directivity functions are proposed for the use in the source description of railway noise. These default directivity functions will be subject to revisions when more accurate data become available.

1. Introduction

In the Harmonoise project railway noise is characterized by three main sources [1]: rolling noise, traction noise and aerodynamic noise. In the source description these noise sources will be defined by their sound power level spectra in one-third octave bands, the vertical and the horizontal directivities, and the speed dependence of the sound power levels. The equivalent noise sources (a few incoherent point sources at different heights, which are fixed as required by the engineering model [1]) are determined from these physical sources (a line/group of incoherent point sources).

In Ref. [2], the directivity functions used in some national models (in Europe) have been reviewed. Some other authors have reported their investigations on the directivity of rolling noise [3–5]. To determine the directivities of railway noise and to have default directivity functions for the use in the Harmonoise engineering model systematic investigations, both with measurements and with model simulations, have been carried out at SP [6–10]. Based on this work the methods to measure and to determine the directivities of railway noise will be presented in this paper. The discussion for rolling noise is given in detail. Discussions for traction noise and aerodynamic noise will be more analytical because of limited access to relevant directivity data.

*Corresponding author. Tel.: +46 33 165021; fax: +46 33 138381.
E-mail address: xuetao.zhang@sp.se (X. Zhang).

0022-460X/$ - see front matter © 2006 Elsevier Ltd. All rights reserved.
doi:10.1016/j.jsv.2005.08.057

For most railway noise sources it can be assumed that the directivity patterns will not vary with the motion of the sources (except the Doppler effect on their spectra). It is then possible to manage directivity measurements with the source being stationary, assuming that the noise can be generated properly. One exception is aerodynamic noise, the directivity of which may vary with train speed. The directivity of aerodynamic noise can be measured during a train pass-by, or, by some wind-tunnel measurements [11]. There is no report on the boundary effect of the wall of a wind tunnel on the directivity.

For stationary noise sources that are small in geometry the directivity can be measured by directly applying EN ISO 3744—to measure sound pressure level distribution on a hemispherical surface. For noise sources that are large in geometry such as a locomotive the vertical directivity may for practical reasons have to be estimated by a less accurate method—to measure sound pressure level distribution on a box-shaped surface. For some noise sources that are extremely large in geometry such as a bridge or a track (in one dimension), there is currently no effective method to measure the directivity.

The consideration behind the choice of method also concerns measurement distances and noise emission levels. To obtain accurate data the signal-to-noise ratio should be high. On the other hand, to determine the directivity of a compound noise source, for which each sub-source may have the same or different directivity characteristics, the measurement distance should not be less than the source dimension; otherwise the measured directivity pattern will vary with the distance [8].

The directivity of train noise is determined by the combined directivity effects of its sub-sources. It can vary from one train to another because of different combinations of sub-sources. It can also vary with train speed because different sub-sources will dominate in different speed ranges. Additionally it will also vary with the measurement distance d when $d < l$ (the train length) [8]. Since the directivity of each incoherent point source will be the same whether or not the other sources exist it can be determined individually. With all the directivities of the sub-sources known the directivity of the total train noise can be predicted [8].

In Sections 2–4 practical methods to determine the directivities of rolling noise, traction noise and aerodynamic noise will be described. Default directivity functions for these three main railway noise sources are also proposed in the relevant sections. Remarks on these default directivity functions are given in Section 5. Relevant literature is given at the end of this paper.

2. Determination of the directivity of rolling noise

Rolling noise consists of wheel noise and track noise. To determine the directivity of rolling noise one needs to know the directivities of wheel noise and track noise.

It has been assumed that the directivity pattern of wheel noise can be different if a wheel is excited vertically or laterally, but will not be affected by how it is excited, i.e. by a shaker or by roughness when the wheel is rolling on a rail. A similar assumption is applied for track noise.

2.1. Directivity of wheel noise

In Europe the diameter of the most popular wheels is about 920 mm (for new wheels), which is small enough for applying EN ISO 3744 so the directivity of sound power from a wheel can be measured using a hemispherical surface which has a radius of at least twice the characteristic source dimension. In fact, only vertical/horizontal circles will be used to measure vertical/horizontal directivity, respectively. One example of the measurement set-up is shown in Fig. 1.

The measured sound pressure levels will in general include two kinds of interference effects: (1) interference between the direct sound and the ground reflected sound and (2) interference between the sounds from different parts of the wheel. These interference effects will distort the information on directivity (*Note*: For a distant receiver the interference effects will disappear at high frequencies due to the small turbulence in air.). Using thick absorbing material on the ground will reduce the first kind of interference, but there is no practical way to exclude the second kind of interference.

It is necessary to understand the measured results properly as the interference effects may distort the information on the directivity. It is better to determine the directivity of the A-weighted total level first, since it

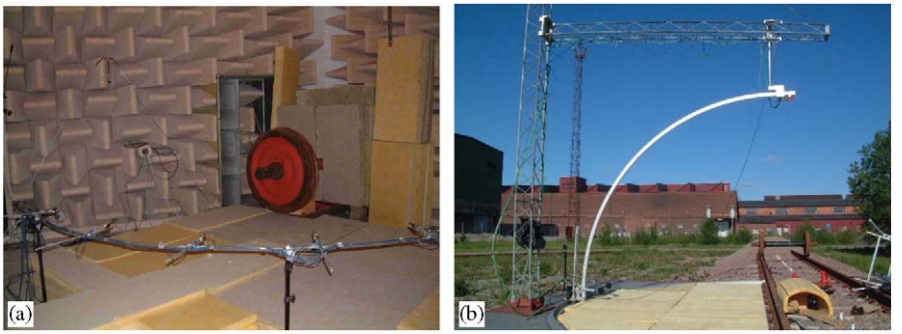

Fig. 1. The set-up for directivity measurements of wheel noise (a) and rail/track noise (b). Mineral wool has been put on the ground to reduce ground reflections.

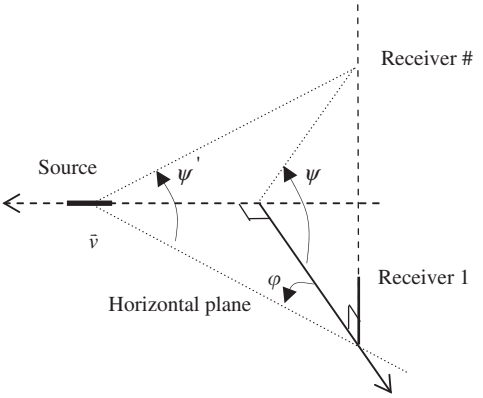

Fig. 2. The definition of angles.

will be less influenced by the interference effects. To determine the directivity in frequency bands two "rules" may apply [6]:

1. Using the envelope of maximum levels (interference peaks), because for two equally strong coherent sources a maximum level will at most be 6 dB higher (than the level by only one of them), but dips can in principle be infinitely low (the sound pressure in some frequency bands could fall close to zero due to interference).
2. There is only a small difference between the directivity patterns in adjacent frequency bands.

Angles are defined in Fig. 2.

In appendix, the simulation functions for the vertical directivities in one-third octave bands have applied the two rules. It is also found that it may be better to measure the directivity of wheel noise using a measurement circle with a radius of about 6 m, because interference between the sounds from different parts of the wheel will vary less with a large radius.

It is reasonable to assume that the vertical directivity and the horizontal directivity of wheel noise is the same because of the rotational symmetry. As shown in Fig. 3 and described in Eq. (1) a wheel will radiate like a monopole but a small directional effect, both in the A-weighted level and in one-third octave bands:

$$\Delta L_{\text{wheel}}(\varphi) = 1 + 10\,\lg[0.4 + 0.6\cos(\varphi)], \tag{1}$$

where 1 is a normalization constant, see Eqs. (10)–(12) and lg indicates logarithm to the base 10.

As shown also in Fig. A.3 in appendix, in detail, wheel noise could be less directional at low frequencies than at high frequencies. Since the interference effects can distort the directivity pattern and the interference between the sounds from different parts of a vibrating wheel can vary with measurement radii until the radius is larger than about 6 m (for 920 mm diameter wheels), no frequency-dependent wheel directivity will be

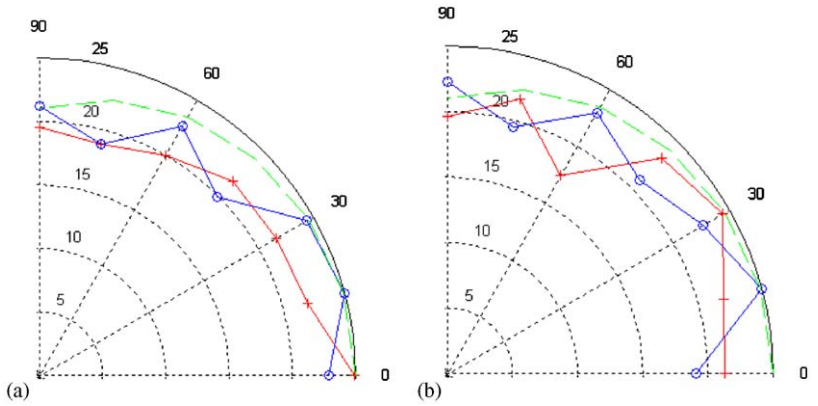

Fig. 3. The directivity of wheel noise (in the A-weighted level), excited vertically and laterally (SJ 57 H freight car wheelset) [6]. (a) Horizontal directivity; —+—, excited laterally; —o—, excited vertically; — —, the simulation, (b) vertical directivity; —+—, excited laterally; —o—, excited vertically; — —, the simulation. (The simulation function is $25+10\lg[0.4+0.6\cos(\psi)]$.)

proposed in this paper because only 2.5 m radius has been used for the relevant measurements. A frequency-dependent description on the directivity of wheel noise will be possible when more data are available.

2.2. Directivity of track noise

The vertical directivity of track noise can be measured in the same way as for the directivity of wheel noise, see Fig. 1(b). When a track is excited vertically, its vertical directivity can be simulated by Eq. (2), for A-weighted total level and (roughly) also for one-third octave frequency bands (Fig. A.1 in appendix).

$$\Delta L_V^{\text{rail}}(\psi) = 10\lg\left[0.4 + 0.6\cos^2(\psi)\right]. \tag{2}$$

When a track is excited laterally, the vertical directivity of it will be a little more directional than this function, both in the total level and in frequency bands (not presented in this paper to avoid redundancy). The horizontal directivity of track noise cannot directly be measured, because track vibrations are in general less damped and thus a vibrating rail will be a line source. In the TWINS model a track is modelled as a combination of monopole and dipole [12]. For a less damped track (track decay rates are frequency dependent and are in usual cases low above about 630 Hz) a dipole description may be good enough [8]. The track decay rates can be determined using the TSI method [13].

2.3. The vertical directivity of rolling noise

Usually source directivity should not include the effect of reflections or shielding of nearby objects. However, there will be situations when nearby objects play an important role on the source directivity and where it may not be convenient to separate them from the source. One such example is the shielding of the car-body that often has a big effect on the vertical directivity.

The effect of car-body on vertical directivity can be measured in the same way as for wheel noise (Fig. 4). The result will depend on how the car-body is designed.

By combining the vertical directivities of wheel noise, track noise and the shielding effect of the car-body, the vertical directivity of rolling noise can be determined. In Ref. [6], it is concluded that the vertical directivity of rolling noise is mainly determined by the shielding effect of the car-body. The vertical directivity data of wheel noise when a car-body is present are shown in Fig. A.2 in appendix. The simulation functions are given in Eq. (3) for the vertical directivity in one-third octave bands and in Eq. (4) for the A-weighted total level.

$$\Delta L_V^R(f,\psi) = 20\lg[1+f/800]\times\lg[0.15+0.85|\cos(\psi)|], \tag{3}$$

$$\Delta L_V^R(\psi) = 10\lg[0.15+0.85|\cos(\psi)|]. \tag{4}$$

Fig. 4. The set-up for measuring the shielding effect of car-body on vertical directivity [6].

Some indices used in this paper are defined as: $\{H,\ V\} = \{\text{Horizontal, Vertical}\}$ and $\{R,\ T,\ A\} = \{\text{Rolling, Traction, Aerodynamic}\}$. The measurement set-up shown in Fig. 4 corresponds to those car bodies which have the smallest shielding effect on wheels, thus it results in the smallest shielding effect and the smallest vertical directivity.

2.4. The horizontal directivity of rolling noise

The horizontal directivity of rolling noise is determined by the horizontal directivities of wheel noise, track noise and the horizontal shielding on wheels (it is usually not important). Since wheel noise can roughly be modelled as a monopole, see Eq. (1), the horizontal directivity of rolling noise is mainly determined by track properties: the higher the damping, the less the directivity (provided that the track noise is important for the overall sound power level).

The horizontal directivity of track noise can be modelled as a dipole. Its importance in the horizontal directivity of rolling noise relative to wheel noise depends on the damping. In Ref. [8], it is shown that for a less damped track its contribution to the total noise is estimated to be about 3 dB more than that by the wheel and then the horizontal directivity of rolling noise can be described as (for the A-weighted total level)

$$\Delta L_H^R(\varphi) = 2.36 + 10\lg\left|0.15 + 0.85\cos^2(\varphi)\right|. \tag{5}$$

This directivity function has been used in some national models [2]. A general form of the horizontal directivity of rolling noise (for the A-weighted total level) is given below

$$10\lg\left|0.15 + 0.85\cos^2(\varphi)\right| \leqslant \Delta L_H^R(\varphi) < 10\lg[0.4 + 0.6\cos(\varphi)]. \tag{6}$$

3. To determine the directivity of traction noise

Traction noise has many sub-sources [14], which can be distributed between the bogie height and the train roof, and also in a large dimension horizontally. For trains with diesel locomotives the dominant traction noise will be diesel engine noise. When only electric locomotives are used noise from the cooling system will usually be the dominant traction noise.

Diesel traction may comprise a number of sources including exhaust noise, inlet noise, turbo charger noise, noise from the carcase of the engine, structure-borne noise radiated by the vehicle body, traction motor noise (including their blowers or integral fans), noise from compressors and cooling fan noise. (The last three are also found with electric traction.) Each source will have its own acoustic characteristics. In addition the mixture of sources will also depend on the operating conditions. For the sound power levels of traction noise a universal formulation does not exist yet due to the complexity of the issue; nor is there such a formulation for its directivity.

The characteristic source dimension for a diesel loco is often too large for practical measurements of its vertical directivity on a hemispherical surface. In such cases approximate estimates can be made using

a box-shaped enveloping surface according to EN ISO 3746. In Ref. [15] one example of this kind of measurements is given, in which $d = 2$ m (the distance from the reference box to a box-shaped measurement surface). The locomotive is stationary on a concrete ground and the engine runs at its full power (900 rev/min). The measured sound pressure level distribution is shown in Fig. 5.

The measured sound pressure level distribution on a box-shaped measurement surface cannot give an accurate directivity but, combining the knowledge of the source locations and their sound power levels, together with theoretical models of radiation from openings and screening, a useful estimate could be obtained. In the example the exhaust located on the roof-centre causes the highest sound pressure level (97 dB). At the two ends the noise levels are about 14 dB lower, which is due to a longer distance from the main noise sources and some screening effect and possible directivity.

For the horizontal directivity it is suggested to measure the sound pressure levels at the angle positions of 0° and $\pm(15^\circ, 30^\circ, 45^\circ, 60^\circ, 75^\circ, 90^\circ)$ with a radius being the same as the locomotive length, where 0° is on the direction of the normal of a locomotive's sidewall and the origin of the coordinate locates at the middle of the locomotive.

The access to the directivity data of traction noise is limited at present. Moreover, the directivity of traction noise could vary with different types of locomotives and different operating conditions. A general directivity description of traction noise requires much effort to determine the sound power levels of the different types of traction noise sources under different operating conditions. The default directivity proposed here is only for the cases where no better information is available.

$$\Delta L_H^T(\varphi) = 1.21 + 10\,\lg[0.31 + 0.69\,\cos(\varphi)], \tag{7}$$

$$\Delta L_V^T(\psi) = 0. \tag{8}$$

Eq. (7) assumes that engine-room openings are primarily located on the sides of the locomotive. For exhausts of diesel locomotives located on the roof $\Delta L_H^T(\varphi) = 0$ should be used for all relevant low-frequency bands. Also, for electric locos and multiple units the noise level above train roof could be a few dB lower than at the sides. The directivity of the noise from a cooling system can be determined in a similar way.

The directivity of braking noise can be measured in the same way as for wheel noise. And, to measure its directivity one should design a special test rig: the measured wheel can be put on a shaft in such a way that it can rotate and be braked down. If possible the shielding effect of the auxiliary equipment of the test rig should be as similar to the condition in use as possible; otherwise the relevant correction should be done.

Until directivity data of braking noise have become available the directivity of it will be assumed to be the same as that of wheel noise, although braking noise has different characteristics from rolling noise.

Long-side1-middle (3m high)			86.2		91.0		92.7		88.7		
Long-side1-top (6m high)		83.3		88.8		92.7		92.0		86.1	
	Left-end (3m high) 77.9		83.9		91.6	Roof + 2m	97.3		90.6		Right-end (3m high) 78.7
Long-side2-top (6m high)		82.2		87.8		92.8		92.6		84.4	
Long-side2-middle (3m high)			86.2		89.6		90.8		86.6		

Fig. 5. The distribution of the A-weighted sound pressure level (L_{pA} in dB) of SP measured D-locomotive noise [15].

4. To determine the directivity of aerodynamic noise

The directivity of aerodynamic noise can be measured in two ways: (1) wind-tunnel measurements with a microphone array covering all interesting angle positions, such as the example in Ref. [11] and (2) pass-by measurements by using a microphone array as described in Sections 4.1 and 4.2 below.

For vertical directivity these two methods are valid only for pass-by (averaged) vertical directivity (note that the vertical angle will vary during a pass-by). To measure instantaneous vertical directivity the measurement radius should not be less than the train length [8]. To include the effect of inter-coach spacings at least two units are required, which means that the shortest train length will be about 45–50 m. Making a vertical microphone array with this large radius is usually not practical.

It is not clear if the boundary of a wind tunnel will have a strong effect on the turbulence formation. There are two aspects that the boundary conditions of a wind-tunnel that differ from real situations: (1) in the real situation the ground moves relative to the train, but for wind-tunnel measurements the ground is stationary relative to the train; (2) in the real situation a train moves in open air, but a wind-tunnel will have a pipe-like wall which may have strong effect on the turbulence formation. One should be careful in using wind-tunnel data as it may give reliable results (if the boundary effect mentioned above is negligible) or it may contain some error (if the boundary effect cannot be neglected). The wind-tunnel results [11] are used in this paper because no other data are available for the time being.

4.1. To measure the (pass-by) vertical directivity

An ideal microphone array for the purpose will form a quarter of circle from the railhead level to the top above the middle line of the track. It should be centred at the nearest rail and have a radius of 10–15 m. Seven microphones (located at angles of 0°, 15°, 30°, 45°, 60°, 75°, 90°) will normally be sufficient. It is possible to use a vertical array if only the wayside range is of concern.

L_{eq} or SEL for the pass-by at different angle positions shall be recorded. After correction for the ground effect, which can be evaluated by the Harmonoise engineering point-to-point model [1], or, the Nord 2000 model [16], the data will give the pass-by vertical directivity. It is recommended to carry out this type of measurements on an elevated track bed (2 m or higher), as the ground effect then will be less sensitive to different angle positions [7].

4.2. To measure the horizontal directivity

Only one microphone position will be used, located at distance d from the track and height h above the local ground.

According to ISO/DIS 1996-2(2003), in order to reduce weather influence, the relationship $(h_s + h_r)/d \geqslant 0.1$ should be fulfilled, where h_s is the height of the source and h_r is the height of the receiver above the ground. As, for train noise, source heights are usually within {0, 6 m} and receiver heights are usually not over 10m, $d < 100$ m will meet the requirements.

As concluded in Ref. [8] the distance d should not be less than the train length l. And, as mentioned above, the shortest train length will be about 45–50 m. Thus, one can choose $d = 50$ m and $h_r \geqslant 5$ m if $l \leqslant 50$ m. Trains with $l > 100$ m are not suitable for the purpose.

One should be careful with sampling time, because for high-speed trains a small time delay could cause a serious error in angle positions. The highest frequencies require a sampling time $t_f \leqslant 1/(2.5 f_{\max})$. The lowest sampling rate will then be $R_f = 1/t_f$. When processing data some kind of time weighting will be applied, this will lower the effective sampling rate. To have data recorded correctly within the angle range it is required to have at least three samples (with equal angle spacing) within any 5° interval. With d the measurement distance and v the speed of the moving source, the effective sampling time is: $t_d \leqslant d \times 5\pi/(3v \times 180)$. (Having $d = 50$ m and $v = 500$ km/h one will have $t_d \approx 0.01$ s, or the effective sampling rate 96 samples/s.)

The time history of the train (centre) position has to be known. The time history, or equivalently, the angle distribution, of the sound pressure level $L_p[\varphi(t)]$ is to be recorded and used in Eq. (11) below to determine the horizontal directivity.

4.3. The formulae for determining the horizontal directivity

The information on the directivity of a passing-by noise source (on a straight track) can be obtained using the difference between the sound exposure levels for the angle ranges $\left(-\frac{\Delta\varphi}{2},\ \frac{\Delta\varphi}{2}\right)$ and $\left(\varphi-\frac{\Delta\varphi}{2},\ \varphi+\frac{\Delta\varphi}{2}\right)$, with $\Delta\varphi$ being a small-angle range [10]. The sound exposure level L_E can be calculated by using the measured sound pressure level $L_p[\varphi(t)]$, as given below

$$L_E(\varphi)=10\lg\left(\int_{\varphi-\Delta\varphi/2}^{\varphi+\Delta\varphi/2}10^{L_p(\varphi)/10}\frac{d}{\cos^2(\varphi)}\,\mathrm{d}\varphi\right)-10\lg(v). \tag{9}$$

It is recommended to choose $\Delta\varphi\leqslant 5/3$ degrees. The normalized directivity $\Delta L(\varphi)$ will be determined using Eq. (9), but with the excess attenuation $A_{\text{excess}}(\varphi)$ compensated, as follows:

$$\Delta L(\varphi)=\Delta L'(\varphi)-10\lg(C), \tag{10}$$

where

$$\Delta L'(\varphi)=10\lg\left(\int_{\varphi-\Delta\varphi/2}^{\varphi+\Delta\varphi/2}10^{[L_p(\varphi)+A_{\text{excess}}(\varphi)]/10}\frac{d}{\cos^2(\varphi)}\,\mathrm{d}\varphi\right)-10\lg\left(\int_{-\Delta\varphi/2}^{\Delta\varphi/2}d^*10^{[L_p(0)+A_{\text{excess}}(0)]/10}\,\mathrm{d}\varphi\right), \tag{11}$$

$$C=\frac{1}{\varphi_{\max}-\varphi_{\min}}\int_{\varphi_{\min}}^{\varphi_{\max}}10^{\Delta L'(\varphi)/10}\,\mathrm{d}\varphi,\quad -\pi/2<\varphi_{\min}<\varphi_{\max}<\pi/2, \tag{12}$$

where $\varphi_{\max}$ should be close to $\pi/2$ and $\varphi_{\min}$ close to $-\pi/2$ such as $(-85^\circ, 85^\circ)$; $\varphi_{\min}$ can be 0 when $\Delta L'(\varphi)$ is symmetric.

To use Eq. (9) the effect of time delay (it takes a finite time for the sound to travel from the source to the receiver) should be corrected for, especially for a long train.

When working in frequency bands the Doppler shift could be tolerated in many cases. For example, taking $c=344\,\mathrm{m/s}$, for a train speed of 100 km/h the perceived frequency will shift about 8% for $\varphi=80^\circ$, 5.7% for $\varphi=45^\circ$ and 1.4% for $\varphi=10^\circ$. Doubling the train speed will double the Doppler shift at these angles. Thus, the Doppler shift has to be considered only for high-speed trains (at large-angle positions).

The basic requirements on measurement conditions are listed here: (1) The track chosen for directivity measurements should be straight, level and long enough in both directions, such as $[-5d, 5d]$. (2) The site should be free from screens and large reflecting objects. (3) The background noise level should be reasonably low. (4) Single pass-by with a constant speed. (5) A roughly flat terrain that has no important angle-variance in shape and in impedance. (6) The favourable propagation conditions (small downwind ($<5\,\mathrm{m/s}$) or the temperature inversion).

4.4. Default directivity

The default vertical directivity of aerodynamic noise is assumed to be negligible. The default horizontal directivity of aerodynamic noise is given by Eq. (13), referring to data given in Ref. [11]

$$\Delta L_H^A(\varphi)=2.37+10\lg[0.01+0.5\cos(\varphi)+0.49\cos^2(\varphi)], \tag{13}$$

$$\Delta L_V^A(\psi)=0. \tag{14}$$

Note: Aerodynamic noise is produced by the dipole and quadrupole layers in the turbulent air flow around train body. But, it is shown in Ref. [11] that the horizontal directivity of aerodynamic noise is possibly a little less directional than a free dipole. And, in Ref. [11] it is also shown that the peak sound power might appear at an acute angle to the direction opposite to the motion of the train, due to the convection motion of the turbulent eddies. It is also possible that the directivity of aerodynamic noise will depend on speed. Eq. (13)

indicates that this directivity is a little less directional than that of a free dipole. The last two features can be added to the default directivity when relevant data become available.

The method can also be applied to determine the horizontal directivity of rolling noise.

In the Harmonoise source model aerodynamic noise has two heights: 4 m for high sources (around the pantograph and the roof) and 0.5 m for low sources (around bogies). Using noise barriers (2 m from track and

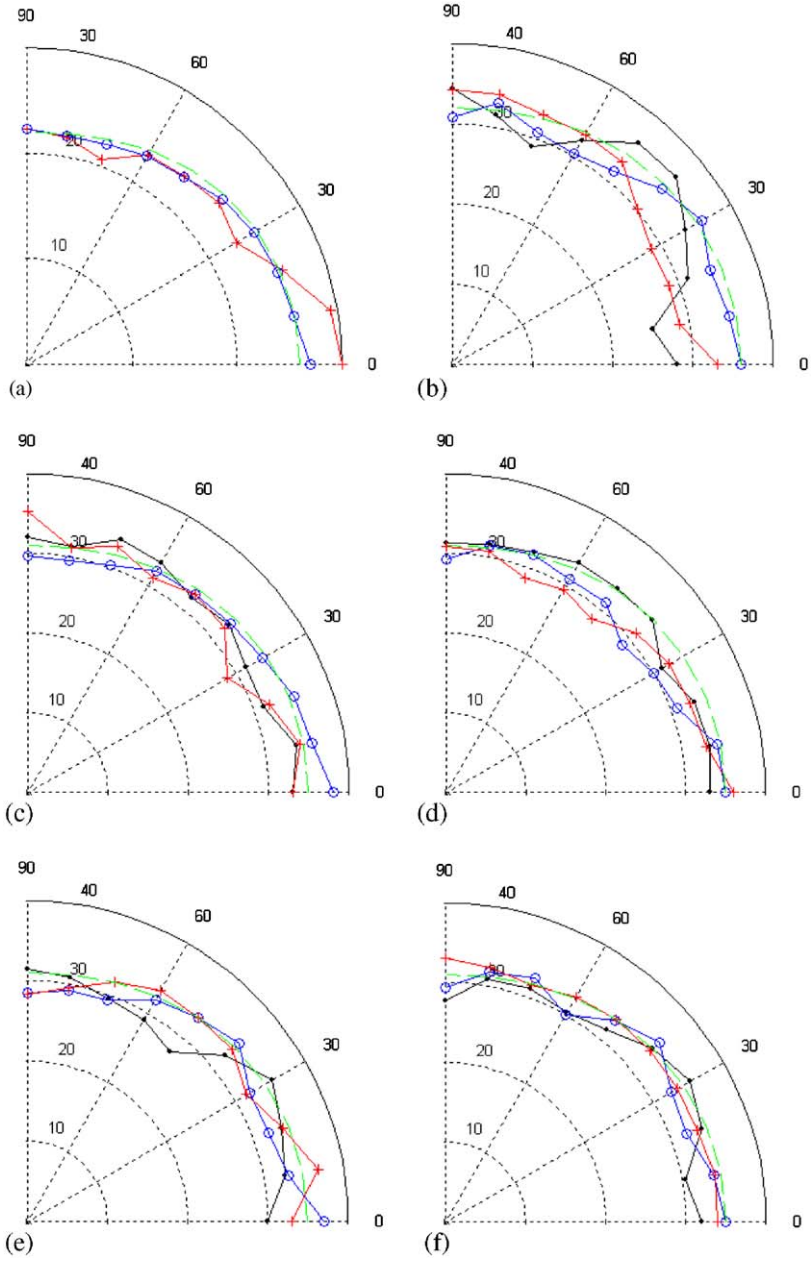

Fig. A.1. The vertical directivity of rail/track noise (rail type: UIC 60) [6]. (a) The directivity of a-weighted total level; —+—, excited laterally; —o—, excited vertically; — —, the simulation function $26+10\lg[0.4+0.6\cos^2(\psi)]$, (b)–(f) the directivities in third-octave bands, excited vertically: (b) —•—, 315 Hz; —o—, 400 Hz; —+—, 500 Hz; — —, the simulation, (c) —•—, 630 Hz; —o—, 800 Hz; —+—, 1000 Hz; — —, the simulation, (d) —•—, 1250 Hz; —o—, 1600 Hz; —+—, 2000 Hz; — —, the simulation, (e) —•—, 2500 Hz; —o—, 3150 Hz; —+—, 4000 Hz; — —, the simulation, (f) —•—, 5000 Hz; —o—, 6300 Hz; —+—8000 Hz; — —, the simulation. (The simulation function is $35+10\lg[0.4+0.6\cos^2(\psi)]$.)

2–3 m above rail) [17] can separate high sources from the low ones. The horizontal directivity of the total aerodynamic noise sources and the horizontal directivity of the high sources can be determined separately, using the separation technique described in Ref. [17]. Thus, the horizontal directivity of the low sources can be deduced.

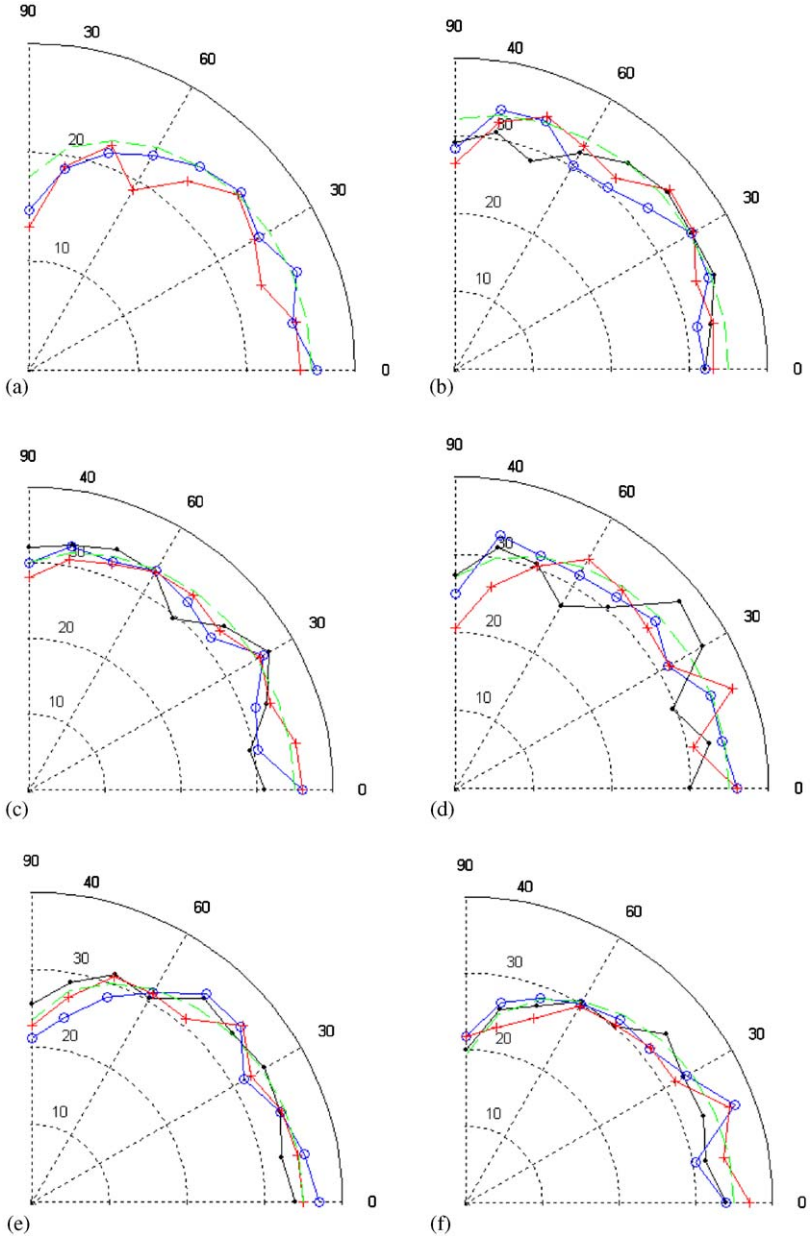

Fig. A.2. The vertical directivity of wheel noise when the "car-body" is put above the wheel (SJ 57H freight car wheelset) [6]. (a) The directivity of A-weighted total level; —|—, excited laterally; —○—, excited vertically; — —, the simulation function $26+10\lg[0.15+0.85\cos(\psi)]$, (b)–(f) the directivities in third-octave bands, excited vertically: (b) —•—, 315 Hz; —○—, 400 Hz; —|—, 500 Hz; — —, the simulation with $f=400$, (c) —•—, 630 Hz; —○—, 800 Hz; —|—, 1000 Hz; — —, the simulation with $f=800$, (d) —•—, 1250 Hz; —○—, 1600 Hz; —|—, 2000 Hz; — —, the simulation with $f=1600$, (e) —•—, 2500 Hz; —○—, 3150 Hz; —|—, 4000 Hz; — —, the simulation with $f=3150$, (f) —•—, 5000 Hz; —○—, 6300 Hz; —|—8000 Hz; — —, the simulation with $f=6300$. (The simulation function is $35+20(1+f/800)\lg[0.15+0.85\cos(\psi)]$.)

5. Remarks

It is desirable to have directivity functions in one-third octave frequency bands, for the use in the Harmonoise engineering model. But, due to the complexity of the problem and the shortage of high-quality data, only the *vertical* directivity of rolling noise can be proposed in one-third octave bands for the time being,

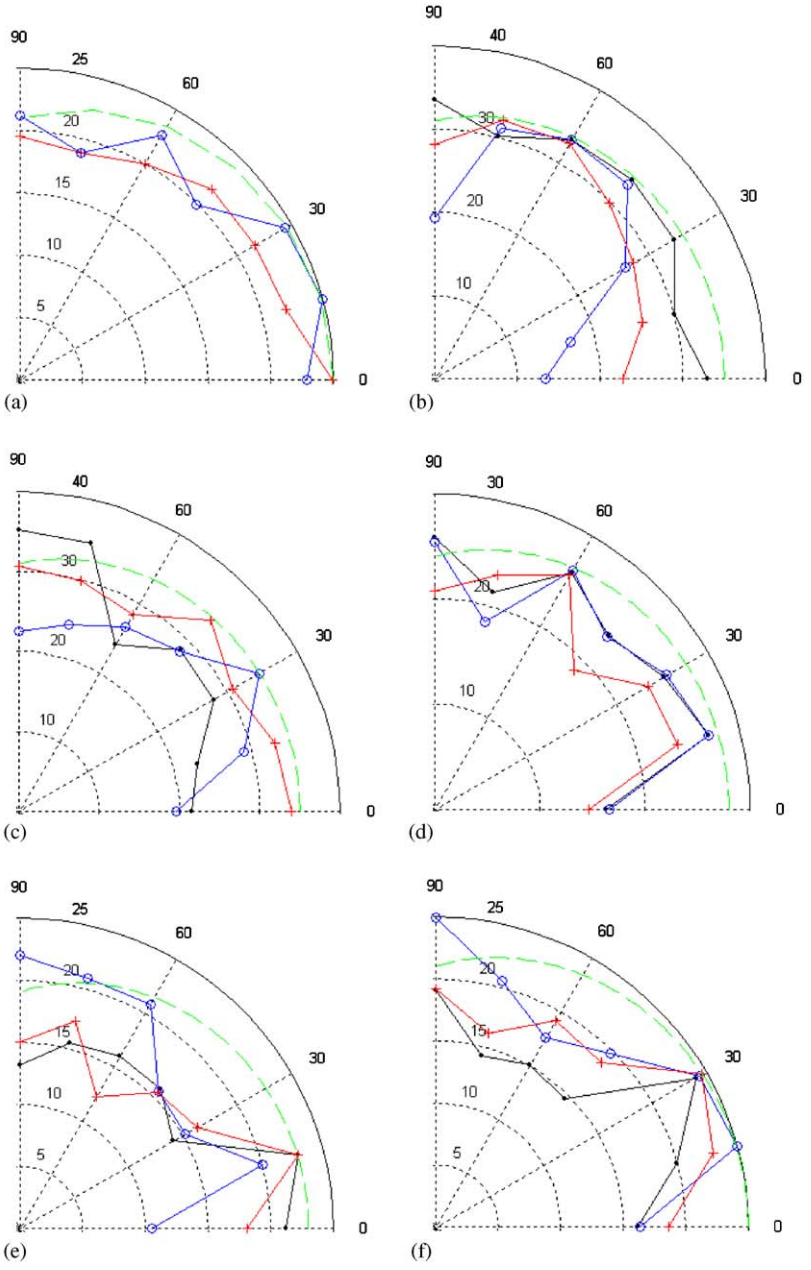

Fig. A.3. The horizontal directivity of wheel noise (SJ 57H freight car wheelset, see Fig. 1). (a) The directivity of A-weighted total level; —|—, excited laterally; —o—, excited vertically; — —, the simulation function $25+10\lg[0.4+0.6\cos(\varphi)]$, (b)–(f) the directivities in third-octave bands, excited vertically: (b) —•—, 315 Hz; —o—, 400 Hz; —|—, 500 Hz; — —, the simulation, (c) —•—, 630 Hz; —o—, 800 Hz; —|—, 1000 Hz; — —, the simulation, (d) —•—, 1250 Hz; —o—, 1600 Hz; —|—, 2000 Hz; — —, the simulation, (e) —•—, 2500 Hz; —o—, 3150 Hz; —|—, 4000 Hz; — —, the simulation, (f) —•—, 5000 Hz; —o—, 6300 Hz; —|—, 8000 Hz; — —, the simulation. (The simulation function is $35+10\lg[0.4+0.6\cos(\psi)]$.)

which is mainly determined by the shielding effect of the car body and is easier to determine than for the other directivity functions. The other default directivity functions are given only for the total A-weighted sound power level.

To have the *horizontal* directivity of rolling noise in one-third octave bands, which is mainly determined by the track decay rates (when track noise is important for the overall sound power) and then will be different in different frequency bands, the proposed methods shown in Sections 4.2 and 4.3 can be applied to obtain high-quality data that can help to reach the purpose.

Similarly, to have one-third octave band directivity functions for traction noise and for aerodynamic noise, high-quality directivity data are needed.

All the default directivity functions proposed in this paper will be subject to revisions when more accurate data become available.

Acknowledgements

The authors are grateful to the two referees for their helpful comments. Most of the work has been carried out within the frame of the Harmonoise project which was supported by the European Commission and the 5th FP (IST).

Appendix. The measured one-third octave band directivity data of rolling noise

The vertical directivity of rail/track noise is shown in Fig. A.1.

The vertical directivity data of wheel noise when a car-body is present is shown in Fig. A.2. The horizontal directivity of wheel noise is presented in Fig. A.3.

References

[1] C.C. Charlet, C. Talotte, P.E. Gautier, Towards an appropriate description of railway noise sources, in: *Euronoise 2003*, paper 527 (the relevant deliverables can be download from: www.harmonoise.nl).
[2] J.J.A. van Leeuwen, M.A. Ouwerkerk, Comparison of some prediction models for railway noise used in Europe, Report L.94.0387.A, DGMR Consulting Engineers bv, The Hague, The Netherlands, 1997, 128pp.
[3] P.J. Remington, Wheel/rail noise—part I: characterization of the wheel/rail dynamic system, *Journal of Sound and Vibration* 46 (3) (1976) 359–379.
[4] T. Ten Wolde, C.J.M. van Ruiten, Sources and mechanisms of wheel/rail noise: state-of-art and recent research, *Journal of Sound and Vibration* 87 (2) (1983) 147–160.
[5] S. Peters, The prediction of railway noise profiles, *Journal of Sound and Vibration* 32 (1) (1974) 87–99.
[6] X. Zhang, Measurements of directivity on test rig, Harmonoise Report HAR12TR-020910-SP04, 2003-04-30.
[7] H. Jonasson, X. Zhang, Modelling of railway noise sources with applications on Swedish trains, SP Report 2001:40.
[8] X. Zhang, To determine the horizontal directivity of a train pass-by, in: *Inter.noise* 2003, paper N627.
[9] H. Jonasson, Memo with comments on measurements of horizontal directivity, Harmonoise Report HAR11MO-030606-SP01.
[10] X. Zhang, Directivity of railway noise sources, Harmonoise Report HAR12TR-031031-SP03, 2004-01-09.
[11] C.K.W. Tam, Intensity, spectrum, and directivity of turbulent boundary layer noise, *Journal of the Acoustical Society of America* 57 (1) (1975) 25–34.
[12] D.J. Thompson, B. Hemsworth, N. Vincent, Experimental validation of the TWINS prediction program for rolling noise, part I: description of the model and method, *Journal of Sound and Vibration* 193 (1) (1996) 123–135.
[13] Directive 2001/16/EC—Interoperability of the trans-European conventional rail system, 23rd November 2004.
[14] M. Dittrich, F. de Beer, X. Zhang, Modelling of railway traction noise for input to rail traffic noise models, Harmonoise Report HAR12TR-030710-TNO01, 2003-08-25.
[15] X. Zhang, Railway traction noise—the state of the art, Harmonoise Report HAR12TR-030530-SP01.
[16] www.delta.dk/C1256ED60044AA49/0/FB4618A71FCEFB73C1256FCB003A616D?OpenDocument.
[17] M. Beier, Measurement protocol for aerodynamic noise sources, HAR12TR-031125-DB01.